Revised Manuscript

TITLE

Humidity effects on a novel eco-friendly chemosensor based on electrospun PANi/PHB nanofibres

AUTHORS

A. Macagnano, V. Perri, E. Zampetti, A. Bearzotti, F. De Cesare

Corresponding Author:

a.macagnano@iia.cnr.it

ABSTRACT

An environmentally friendly conductive sensor to measure gases and volatile organic compounds (VOCs) in moistened environments, has been designed and fabricated. To achieve this goal, a biodegradable electrospun nanofibrous scaffold based on a polymer blend containing polyaniline and poly-3-hydroxybutirrate (PANi/PHB) has been employed. Several fabrics composed of distinct proportions of the two polymers have been tested. Morphology, electrical parameters and sensing features of the biodegradable nanofibrous layers have been investigated. The nanofibrous layers obtained through electrospinning technology carried out directly on chemoresistors resulted in highly porous membranes and the potentials of such blended scaffolds have been analysed, focusing the attention on the influence of humidity on the features of the resulting sensors, also in terms of reproducibility and stability of their responses. Sensor responses to ammonia and further two chemical compounds differently interacting with PANi (i.e. triethylamine and acetic acid) have been measured in dry air and at different percentages of relative humidity, in order to assess in possible applications the influence of PHB in the interactions of PANi with the analytes tested. Due to the properties of the electrospun nanofibres used in these chemoresistors, water vapours seemed to hugely improve the chemical interactions

with the selected analytes. This effect suggests a potential use of the proposed chemosensors in monitoring also strongly moist environments.

1.INTRODUCTION

As a consequence of industrialisation and urbanisation processes, and the employment of modern agricultural practices, gaseous and liquid pollutants are ubiquitous throughout the world and accumulate in ecosystems, thus generating great concerns and warnings for their relationships with human health diseases. In a recent report, WHO stated that in 2012 about 7 million people died as a result of air pollution exposure. This result suggests that air pollution is now the world's main environmental health risk **[1-3]**. Consequently, the monitoring of contaminants in environments is of utmost significance. The emerging technologies have a paramount potential to achieve this goal successfully. Smart devices integrated into the everyday surroundings, usable anytime and anywhere and capable of providing qualitative and quantitative information about pollutants, are increasingly becoming significant for each individual as well as for policy makers to protect populations from pollution exposure. From smartphone embedded sensors to those you wear or plug in wherever you are, this new wave of personal environmental sensors has the potential to really change the way data are gathered, analyzed and used. Alike, the abnormal production of electronic and smart sensing devices begins to represent a significant additional source of pollution to the environment. Although compared to the global production and consumption of plastics in the world, the electronics market (displays, transistors, microelectronic interfaces, cables, cases, etc.) contributes only a small amount of waste, its contribution should not be neglected **[4]**. The consideration of biodegradability and sustainability of electronic-based consumer devices is still in its infancy at present, even if recent demonstrations of high performance organic electronics based on biomaterials have shown that truly 'green' electronics have potential and, hopefully, are poised to make a positive impact in the future. Recently in literature, a demonstration of high performance monitoring systems fabricated on a sacrificial PVA substrate has been reported by John Rogers's group, which developed a collection of multifunctional sensors for physiological measurement (*i.e.* temperature, strain and

electrophysiological) on the surface of a thin PDMS foil on top of a sacrificial water soluble PVA sheet, which served as a temporary support for the transport and mounting of the device onto the skin, as a tattoo **[5,6]**. The sensing system adhering to the skin was working until the beginning of the degradation determined by perspiration and cell regeneration. Since commonly gas and volatile organic compounds (VOCs) sensors consist of a transducer with an interacting chemical layer (the recognition element), if biodegradable circuits could be printed on sheets of silicon so thin that they dissolve in water (from a couple days to a week of submersion), or on natural biodegradable resins, the sensing layer might be degraded, too, thus preventing its persistence in the environment for generations (plastics normally biodegrade very slowly, with full degradation occurring after 500 or 1000 years) **[6-8]**. Specifically among the several potential applications of biodegradable sensors, the monitoring of environmental conditions after ecological disasters, such as oil spills, would result extremely suitable and environmentally friendly if small sensors might be dispersed over a wide area without further contributing to pollution. Similarly, they might be used in sustainable agriculture by monitoring nutrients (like nitrogen, phosphorus and potassium) and water in soil to adapt fertilizers and water managements to crop demands, in order to increase agricultural productivity and maximise farm profitability, while minimising environmental damages. In medicine, implantable sensors would have a wide variety of medical uses, such as tracking blood sugar levels in diabetes patients. Additional to the operation to implant such small devices, which is a non-invasive process, the elimination of the sensors removal process might be very attractive for both patients (who will feel safer, at least because not undergoing another operation), researchers and investors. Although biodegradability is a remarkable feature to have environmentally and health friendly sensing tools, sensors for gas monitoring should be able to preserve their sensing feature for a period of time, despite short, and have reasonable operative shelf life, relative to the specific application and the period to monitor, and should not be then water soluble. Additionally, the sensing material should not be strongly affected or corrupted by environmental parameters, such as temperature and moisture. Among these materials,

the most used for gas sensing are expected to be semiconductors organics, that are inexpensive and their electrical measurements, occurring at room temperature, require simple DC. They can respond to a wide range of polar and nonpolar gases and vapours depending on various interaction mechanisms. For instance, the analyte can affect the charge transfer between the sensing layer and the electrode contact or change the density of charge carriers (due to oxidising or reducing reactions), or change the carrier mobility thus affecting the resistivity of the film. This study focuses on creating and investigating an environmentally friendly conductive sensor for gases and VOCs based on conductive and biodegradable electrospun nanofibres. To achieve this goal, nanofibrous layers at various concentrations of polyaniline (PANi) hosted in a biodegradable polymer of poly-3-hydroxybutyrate (PHB) have been tested. To our knowledge, PANi/PHB nanofibres have never been tested in sensing application, until now. Therefore, electrical parameters of conductive sensors based on nanofibrous layers of PHB hosting increasing concentrations of PANi have been investigated for one year. Fibres have been assembled as highly porous membranes by electrospinning technology **[9]** directly on the transducers. More recently, biocompatibility and toxicity of polyaniline salt and base in environment have been investigated and measured in several studies **[10-13]**. The resulting findings suggested that polyaniline is a biocompatible polymer and its toxicity is strictly related to its concentration (≥400 mgL^{-1}). PANi is the most fascinating molecule among CPs for chemical sensing because it is environmentally stable, easily synthesised, and can react with chemical species at room temperature **[14]**. Its sensing features can be easily tuned for specific applications by modulating the doping process and the hosting polymers, which are mainly responsible for the conductivity and gas/VOCs surface adsorption and diffusion of the resulting material, respectively. PANi becomes an electrically conductive material when the emeraldine oxidation state is doped with an acid that protonates the iminic nitrogen on the polymer backbone. Doping and undoping processes are the key actions in the sensing mechanism of the polymer. Polyaniline is extremely sensitive to ammonia: the interaction with ammonia, causes a dedoping effect through deprotonation. The transfer of protons from PANi -NH- groups to NH_3 molecules

forms ammonium ions and reverts PANi to its base, the less conductive form. On the contrary, acidic gases such as HCl, H_2S, and CO_2, in the presence of water, dope it through protonation, thus increasing PANi conductivity. All these processes are expected to be reversible **[15].** Nanofibres of PANi blended with several polymer carriers have been investigated **[16-18]** for a multitude of applications (healthcare, filtration, biotechnology, energy generation, etc.), thus suggesting their commercial potentiality **[19]**. In these studies, the porous nature of these films, which enabled gas molecules to diffuse in and out of the fibres quickly shortening the doping and dedoping processes. As a consequence, the increased performances of PANi-NF films in both sensitivity and response time, relative to their conventional bulk counterpart, were due to higher effective surface area and shorter penetration depth for target molecules. Nanofibrous layers of PANi hosted in different electrospinnable polymers (polystyrene — PS, polyvinylpyrrolidone — PVP, and polyethylene oxide — PEO) were tested as sensors of gases relevant for human health and disease diagnosis **[20]** or of toxic gases **[21]** and VOCs present in environments to point out ecological risks in order to achieve sensitivities hardly attained with comparable sensing systems. Host polymer carriers resulted responsible of great alterations to the topology of the interacting surface (diameter and length of the fibres, porosity, roughness, presence of beads and grains, non-woven framework and branched junctions, adhesion, etc.), additionally to the modified affinity towards the analytes. In literature conductive devices based on nanofibres of PANi blended to biodegradable polymers like polylactic acid (PLA) were developed and used to sense alcohol vapours of increasing molecular size **[22]** enhancing the contribution of PLA in the sensor feature. High selectivity to hydrogen gas **[23]** was achieved through a sensor based on PANi embedded in chitosan matrix, which acted as a filter for large size and polar molecules. Polyaniline grains growth onto fibres of bacterial cellulose (PANI/BC) exhibited excellent electrical conductivity (the highest value was 5.0×10^{-2} S/cm) and good mechanical properties (Young's modulus: 5.6 GP, tensile strength: 95.7 MPa) suggesting potential applications in flexible sensors **[24]**. Electrospun fibres of silk coated by polyaniline were investigated also as suitable sensing material for electrochemical

sensors in liquid, capable to detect an electrolyte (i.e. methanesulfonic acid) in solution[**25**]. Electrospinning was utilised too to synthesise a polyaniline (PANI)/poly(ε-caprolactone) (PCL) blend in the form of nanofibres in order to examine its gas sensing performance to water vapour, NH_3, and NO_2 **[26]**, where the sensitivities to analytes were modified changing the acid doping. In the present study, PHB has been selected, as biodegradable polymers, because it is water insoluble and relatively resistant to hydrolytic degradation: these features differentiate PHB from most other currently available biodegradable plastics, which are either water soluble or moisture sensitive, i.e. mostly useless in sensing applications. Additionally, PHB is known to be permeable to oxygen, to be UV and thermal resistant, to have noteworthy tensile strength (40 Mpa), to be biocompatible and non toxic. Such features make this material as a promising candidate for biodegradable sensors. PHB is a polyhydroxyalkanoate produced by microorganisms (*Ralstonia euthrophus, Bacillus megaterium, Methylbacterium rhodesianum*), apparently in response to conditions of physiological stress, such as limited nutrition **[27]**. Commonly, this polymer is used in medicine for its biocompatibility (surgery and surgical implants, blood vessels) as well as in pharmacy (microcapsules, tablets packaging), because also its biodegradation products are non-toxic. It may be functionalised on purpose or mixed with suitable chemical compounds to make it chemically attractive as a sensor. In literature, nanofibres of biodegradable poly(3-hydroxybutyrate) blends having 8 to 55% acid-doped polyaniline (70–100 nm in diameter) have been prepared and their biodegradability investigated **[28]**. The most common electrodes used for manufacturing conductometric sensors are interdigitated electrodes (IDEs) that are implemented over insulating and flat substrates (like alumina, silicon dioxide wafers, etc.) in various geometrical layout (one or several pair of electrodes) using photolithography and metal deposition techniques. A constant potential is applied and the output signal strength of IDEs is controlled by the design of the active area, width and spacing of the electrode fingers. The resistance value depends on both the quantity and quality of the texture covering the electrodes, such as fibre density, shape and dimension of fibres (individual resistance value) assembled over the electrodes (aligned, nonwoven, etc.). The potentials

of such blended polymers have been exploited, focusing the attention on the influence of humidity on the features of the resulting sensors, also in terms of reproducibility and stability of their responses. Indeed the presence of water vapour, functioning as interference gas, was expected to lower the gas response of the sensor in a humid atmosphere **[29]**. Briefly, the responses of these PANi/PHB sensors to ammonia in trace were measured in dry air and at different percentages of relative humidity, in order to evaluate the role of PHB in the interactions of PANi with the gas in actual applications. Similarly, the effects of distinct moisture conditions on the responses and sensing features of PANi/PHB sensors to both acidic and basic VOCs (i.e. acetic acid and triethylamine, respectively) were investigated.

2.MATERIALS AND METHODS

Polyaniline emeraldine base (PANiEb, 10,000 MW), 10-camphorsulfonic acid (CSA), Poly[(R)-3-hydroxybutyric acid, PHB] and 2,2,2-Trifluoroethanol (TFE) were all purchased from Sigma-Aldrich and used without further purification.

A milky PHB solution (PHB_{sol}) was prepared solving 5% (w/w) polymer in TFE under magnetic stirring at 60°C (≥72 h). A conductive solution of PANiEb, specifically doped with CSA (300:200 mg PANiEb:CSA or PANi) and dissolved in TFE (20 ml) under magnetic stirring at room temperature (≥24 h) was also prepared. The resulting deep-green solution was filtered through 1 μm pore size PTFE membrane filter (Millipore) to get a more homogeneous solution ($PANi_{sol}$). Filtering membranes were then dried and weighed, and their contribution in terms of the only PANi weight was subtracted to the initial PANi amount (the kept PANi resulted less than 2%). Six polymer blend solutions were prepared by mixing increasing volumes of $PANi_{sol}$ (hundreds microliters) into a fixed volume of PHB_{sol} (1 mL,~24h), in order to obtain PANiEb:PHB mass ratios (w/w) of 1.4%, 2.7%, 4%, 5.45%, 8% and 11%, which were named as the first six letters of the alphabet (A-F), respectively.

The transducers used to convert the physicochemical interactions of analytes with the polymer fibres in electrical signals were interdigitated electrodes (IDEs) **[30]** designed and manufactured in CNR (Italy) on oxidised silicon wafer through a standard

photolithographic process (lift-off procedure **[31]**) followed by the evaporation of a chromium–gold layer. They comprised 40 pairs of electrodes (150 nm in electrode thickness, 20 μm in gap and electrode width and 5620 μm in length). After electrospinning coating, all electrical signals of the resulting chemoresistors were recorded through an electrometer (Keithley 6517 Electrometer).

The electrospinning apparatus used in the present study consisted of a high power AC-DC (alternative current-direct current) converter, a high voltage oscillator (100 V) driving a high voltage (ranging from 1 to 50 kV), a syringe pump (Model KDS 200, KD Scientific) and a rotating conductive cylinder with a diameter of 45 mm. The fibrous layers were fabricated by applying 7-9 kV range of electrostatic DC voltage (depending on the PANi concentration) between the tip of 1 cm long stainless steel in a syringe pump (100 μl h^{-1} in feed rate) and the transducer placed on the grounded collector, opposite to the syringe pump, at 15 cm distance. The depositions were carried out in a home-made clean box equipped with temperature and humidity sensors, deposition time was fixed at 20 min for all polymer materials (in order to obtain a good coverage of the electrodes), the rotation speed was set to 1000 rpm and depositions were carried out at about 21°C and 30% RH (relative humidity).

The nanofibrous materials were optically investigated through scanning electron microscopy (SEM Jeol, JSM 5200, 20 keV, X4500 MAG, gold film), and transmission electron microscopy (TEM Jeol, JEM 1200 EXII).

Water contact angles (WCA) measurements were provided by a USB Digital Microscope Logitech and Image J Free Software. The chemoresistors (IDEs) were placed in a measurement chamber (2.5 ml internal volume) made from PTFE and equipped with temperature and humidity sensors (Honeywell HIH 3602 C). Each IDE was linked to the electrometer to measure the current flowing through the IDE (DC) when a fixed potential was applied to it. Dynamic measurements were carried out at room temperature using both a 4-channel MKS 247 managing four MKS mass flow controllers, set in the range 0–200 sccm (standard cubic centimetres per minute), with an accuracy greater than 1% at

maximum flow, and an Environics S4004 system managing two mass flow controllers set in the range 10-1000 sccm and 0-50 sccm, respectively.

Synthetic dry air (5.0) was used as carrier gas (provided by Praxair-Rivoira, Italy) and was blended with ammonia from cylinders at fixed concentrations (10 ppm mol^{-1} in N_2, provided by Praxair-Rivoira, Italy) in order to test the dependency of IDE responses on gas concentrations. To test the interaction of water on the electrical properties of different polymer blends after electrospinning deposition and interaction with ammonia, humidified dilution air was prepared by running the dry atmospheric air through an H_2O bubbler containing demineralised water in order to obtain distinct percentages of water vapours. Similarly, acetic acid and trimethylamine vapours (VOCs) were diluted with dry and humidified air by using mass flow controllers at room temperature (20°C).

The total gas flow passing through the measurement chamber, housing the IDEs, was set at constant 300 sccm. Each measurement was performed by flushing analytes of interest in the measurement chamber for suitable periods, according to the information to get and the specific features of analytes to test, and then cleaning sensor surfaces with air carrier gas until the complete recovery of the starting current (the baseline). IDE responses were calculated as both current (I) and normalised current (I/I_0), where I denotes the current and I_0 the current under carrier gas flow before the analyte exposure.

3.RESULTS AND DISCUSSION

The nanofibrous fabrics obtained from electrospinning deposition showed several shades of green, dependently on the amount of PANI: the most intense green corresponded to the highest PANi concentrations (E-F) (Figure 1,*ab*).

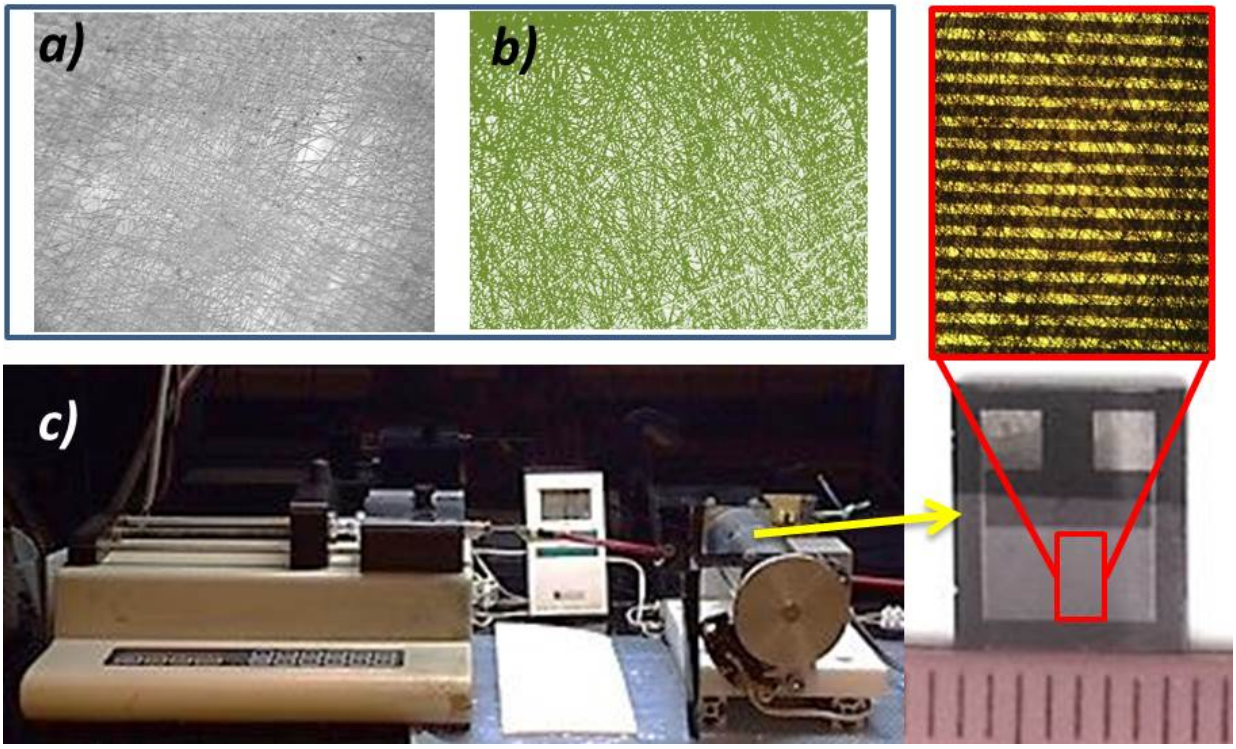

Figure 1. Optical micrographs of the nanofibrous layers called A (*a*) and F(*b*), respectively, coating microscope glass slides; (*c*) a picture of CNR-IIA home-made electrospinning equipment comprising a rotating collector where transducers were placed for deposition. The yellow arrow points to an interdigitated electrode after an electrospun deposition, where a rectangular area was magnified by optical micrograph (red framed).

A dense network of continuous nanofibres covering the sensing area of the interdigitated electrodes (i.e. the area comprising the gaps and the metal fingers) was observed in all of the chemosensors created with the diverse polymer solutions employed (Figure 1,c). The electrospun scaffolds were characterised by high porosity deriving from both enhanced presence of openings and interconnected void volumes, and high surface-to-volume ratios (specific surface area) originating from quite small nanofibres diameters. These key features make such nanostructured fabrics potentially appealing in chemical sensing. SEM micrographs of silicon wafers coated with the electrospun nanofibrous layers of PANi/PHB blends at several mass ratios highlight the high degree of pores and interconnected void volumes, as well as the wide range of fibres diameters (Figure 2).

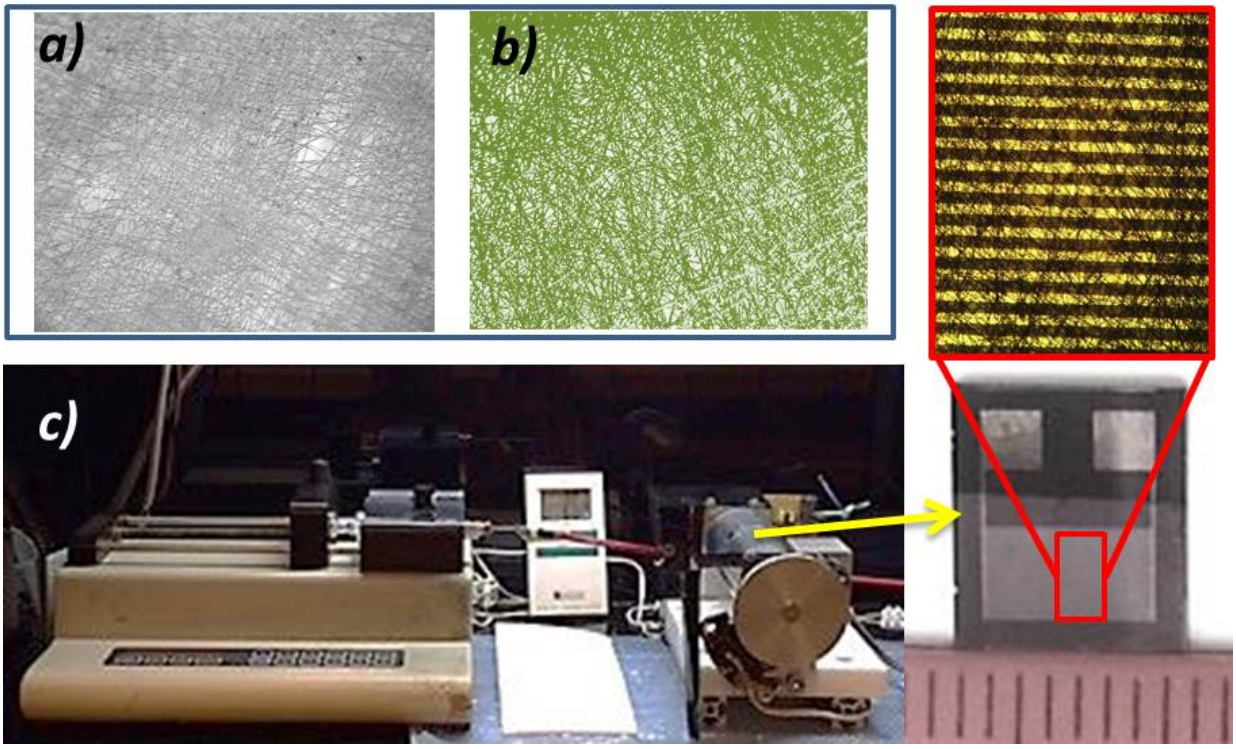

Figure 2. SEM micrographs show PANi/PHB nanofibers coating silicon wafers at increasing PANi mass ratios (A:1.4%, D:5.45%, E: 8%, F:11%).

Additionally, very slight differences in textures quality and size of fibres can be observed among nanofibres obtained with B, C and D blends, i.e. in samples where small volumes of polyaniline were added to PHB. Therefore in Figure 2 only the micrograph of D will be presented. Specifically, fibres resulting from PANi/PHB blend with the smallest amount of PANi appeared branched, with a wide range of size distribution of the fibres (A, in Fig.2), from a few nanometres to hundreds nanometres and 150 nm as mean value. By contrast, D-F fabrics looked uneven in shape, lumpy and with more roughness, but fibres were more homogeneous in size and slightly increased in diameter mean (~200nm). The morphology of the resulting fibres was presumably depending on the different parameters of the starting solutions, such as blend conductivity, superficial tension and viscosity deriving from the increasing amounts of the non-electrospinnable PANi solution (the conducting polymer) **[32]**. In the electrospinning process, it is known that by tuning several parameters such as the viscosity of polymer mixture, the nozzle-ground distance and the potential applied, fibre quality can be modified. In the present study, the

diminished concentration of the insulating polymer, which generally increases its electrospinnability, decreased the viscosity of polymer mixtures. This result caused a substantial increase in the electrical performances (higher conductivity) and reproducibility probably due to the better adhesion onto the metal electrodes observed in the more conductive solutions, despite the not perfectly regular shape of the fibres. Furthermore, taking into account that: i) the longer the distance between needle and collector (longer time of flight), the less the reproducibility of the deposition technique, because of both the instability of the jet and the small dimensions of the transducers housed in the collector; ii) the shorter the distance, the larger the diameter of the fibres produced and the larger the number of globular structures along the fibres, then the distance between needle and collector was set at 15 cm. TEM bright field micrographs reported in Figure 3 show thin web-like and branched structures becoming darker depending on the increase of PANi concentration, presumably due to the greater electron density of this polymer relative to PHB. In scientific literature it is reported that it is possible to identify, in a core-shell fibres observed under TEM, the presence of a core polymer in a sheath of other polymers through sharp boundaries inside the fibres. These sharp boundaries reflect the difference between the core and shell materials ability for electron transmission **[33,34]**. On the other hand since thicker fibres appear darker in TEM analysis, the change in brightness could also be due to the fibres thickness variation. Nevertheless PHB fibres appeared homogenous in colour (data not shown) but with darker patches when PANI was added (Figure 3, sample A). Such gradual darkening of the fibres when PANi concentration increased, let suppose a relationship between the two polymers used and the brightness. Both polymers could be distinguished within the fibres for their different electron density. Indeed, the electron beam travelling through the specimen under study are scattered and disappear from the beam depending on the density of the polymer materials present in the nanofibres (related to their molecular weights), thus resulting in a different brightness and lightness. The presence of darker areas in tiny fibres of sample A similar to the electron density (darkness) of the thicker ones suggests a discontinuous distribution of PANi during electrospinning deposition. With the increasing of both fibres

thickness and PANi content (D-F), fibres appeared more evenly dark coloured (even the thinner fibres), suggesting a more uniform distribution of PANi throughout the fibres, more concentrated within the bulges and roughness of the surface. Further investigation should be performed to confirm the distribution of such a conductive polymer in the blended fibres.

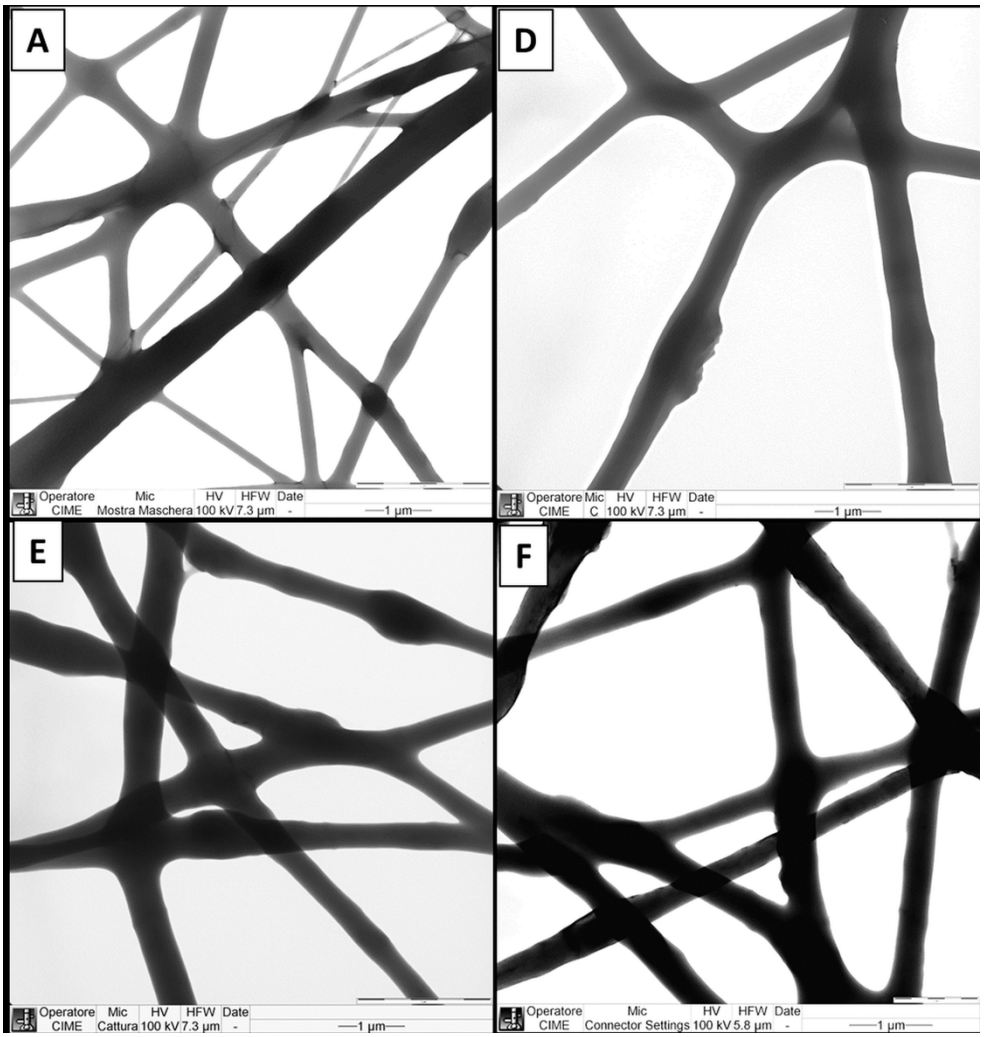

Figure 3. TEM micrographs show A, D, E and F samples, contrasted with uranyl acetate.

The electrical parameters of the resulting fibrous layers were tested by measuring the current variations (Ampere) when voltage was changed (Volts). Figure 4 reports the current–voltage curves of the resulting chemosensors (named A, B, C, D, E, F) in dry conditions (under air flow). The linear shapes within the selected voltage range (−2 V to +2 V) showed constant resistance values for all of the polymer blends, suggesting a good

adherence of the polymers to the gold electrodes additionally to Ohmic conductivity to the fibres already at the lowest concentrations of PANI **[35,36]**. Pristine PHB fibrous layers with an applied potential set to 3 V were measured too, but current values of 10^{-12} A were recorded.

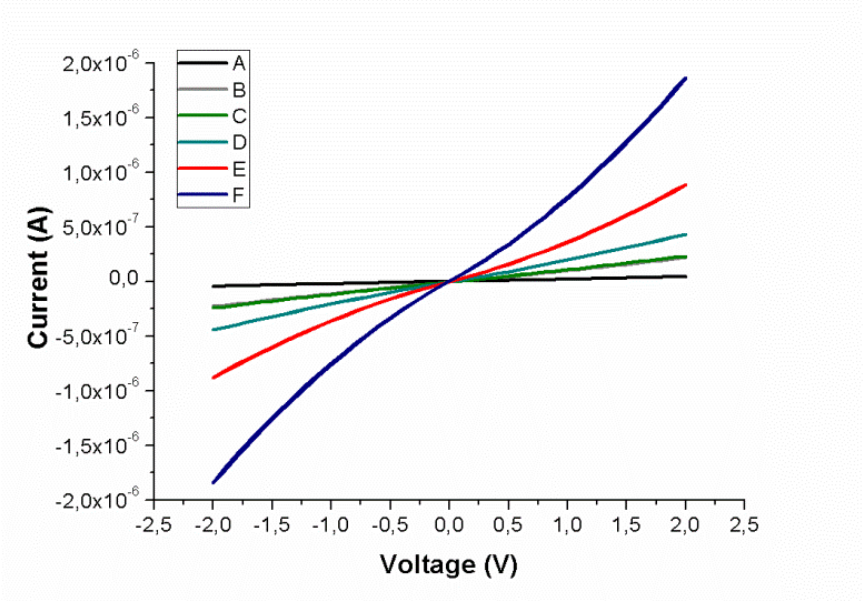

Figure 4. Current-Voltage curves of all the PANi/PHB sensors (A, B, C, D, E, F) between -2 V and +2 V in dry air.

However the resulting measured electrical resistance (Figure 5, a), related to both the individual fibre resistance (dimension and shape) and the fibre density (number of fibres per unit of surface area), showed a negative exponential-like relationships to PANi linear increasing percentage in the fibrous layers. This result apparently suggests a deep relationship between the PANi concentration and its distribution within the fibrous layers, with a threshold value estimated about 2.5 % (PANi:PHB, w:w). Below that, PANi polymer chains should be unhomogeneously distributed within fibres, affecting the conductivity of the layers that generated electrical signals extremely noisy (sample A, data not shown) at the low voltage applied (up to 3V).

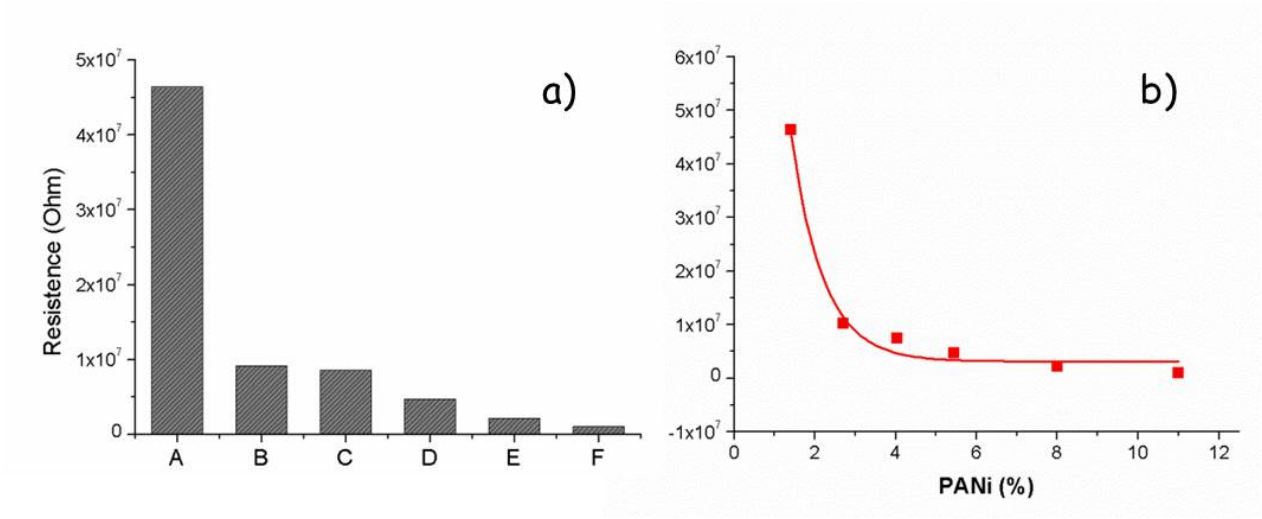

Figure 5. Electrical parameters of the investigated chemosensors; a) bar plot of electrical resistance values of the nanofibrous sensors; b) curve fitting of the electrical resistance values vs PANi/PHB mass ratio in percentage.

The sensor measurements, that were the electrical signals reported when interaction between the sensing layers and the analytes were happening, resulted in a change of the whole resistance (or current, i.e. I=V/R according to Ohm law) of the device according to the following Equation 1 **[33]**:

$$R = \frac{1}{2N-1}\rho\frac{w}{h \bullet L} \quad (1)$$

where *N* and *L* are number and size of the fingers, *h* and *w* the electrode thickness and width, respectively, and ρ la resistivity of the overlying material. Firstly, the chemosensors were exposed to water vapours ranging between 10-60% RH. Each measurement was carried out for 10 min. The relative humidity percentage was measured through a commercial sensor, placed inside the measurement chamber, confirming the achievement of the equilibrium one minute after the start of measurement. The resulting responses to humidity of the investigated sensors showed current increases, although with different slopes (Figure 6) depending on the concentration of PANi. Indeed, the interaction mechanisms at the polymeric surface of PANi/PHB fibres with water vapours can be a lot and opposite. For instance, the high dielectric constant of water for example, can interact

with the N atoms of PANi, thus inducing an extension of the PANi chains into more stretching conformations and generating an increase in the crystallinity of the polymer with a decrease in its electric resistance.

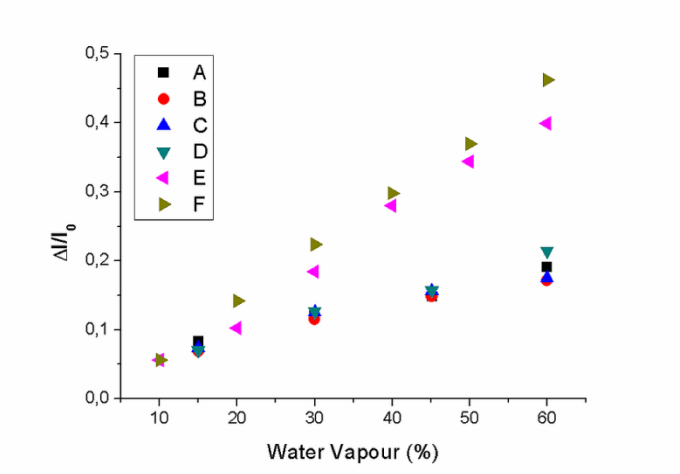

Figure 6. Response curves of PANi/PHB nanofibrous chemosensors to increasing percentages of relative humidity (% RH), ranging between 10%-60% (V=+2 V). For each sensor, the current values (I) were normalized to the starting current values (I_0) before the measuring, in order to be compared.

Additionally also H-bonds between water molecules and N atoms of PANi can induce an increase in current (ie. electrical resistance decrease). Vice versa, water vapour can also dissolve the doping salt (CSA), thus dedoping the molecules and leading to a decrease in current. Finally, a high concentration of water vapour is able to produce swelling of the hosting polymers, spacing out the PANi chains and causing current lowering **[20]**. Since the resulting sensitivity to water vapour, measured as the slope of the normalised sensor responses (I/I_0) to ppm of water vapours (Table 1), increased with PANi concentration, the effects of humidity on PANi/PHB fibres were supposed to be significantly depending on the PANi chains. Although PHB and PANi fibres are known as hydrophobic materials in their nature, there still would have a chance of water penetration because of the interstitial spaces between fibres (pores). Data obtained from WCA (water contact angle) measurements are in very close agreement with the commonly known fact which indicates the following: for hydrophobic surfaces WCA increases with surface roughness and for hydrophilic surfaces, in contrast, WCA decreases with surface roughness **[37]**. In Figure 7,

WCA measurements of A, D and F samples were 90°, 81° e 79°, respectively, confirmed the increase in roughness such as the wettability of the samples with higher PANi concentration.

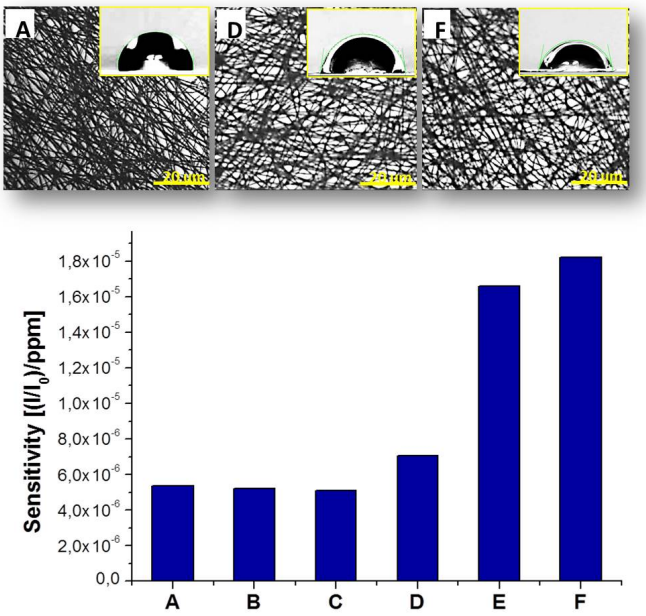

Figure 7. *Top:* WCA pictures of the A, D and F samples captured by a digital microscope and an optical microscope. *Bottom:* bar-plot of the sensitivity (*S*) of the sensors to water vapours concentrations (*ppm*), measured as the slope of the linear fitting of the normalised response curve of each sensor (I/I_0), i.e. $S = (I/I_0)/C$

These results suggested a possible effect of moisture to gas/VOCs interactions. For what concerns the measurements of gas and the effects of moisture on them, the most conductive chemosensors were selected, since able to detect low concentrations of the analytes. Current-Voltage curves of E and F samples reported the huge increase in current (Figure 8), overall in F increased more than twice (F=2.55 x; E=1.26 x), when measurements were carried out in a moist environment (70% RH), presumably due to the water molecules that, adhering on the surfaces, were able to create a thin layer on the fibres and among pores.

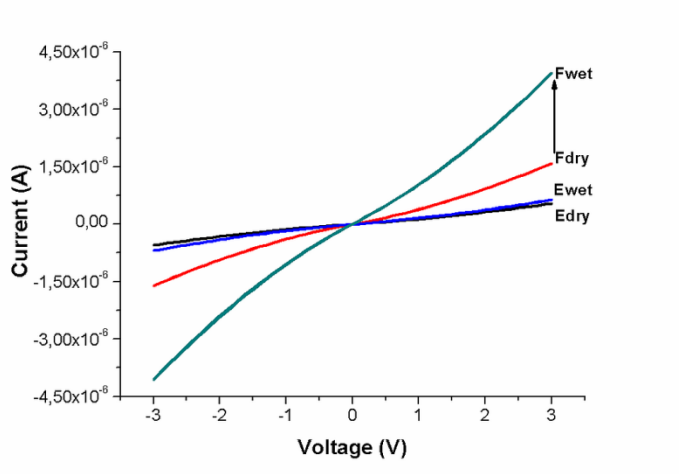

Figure 8. Current-Voltage curves (-3 V ;+ 3 V) of the sensors named E and F under flow of both dry and humidified air.

Table 1. Sensor sensitivity to relative humidity

Chemosensors	Sensitivity (ppm^{-1})	St. Error	R-Square
A (PANi 1.4%)	2.34E-3	±1,2831E-4	0.99
B (PANi 2.7%)	2.27E-3	±2.5204E-4	0,96
C (PANi 4%)	2.23E-3	±3.5832E-4	0.93
D (PANi 5.45%)	3.08E-3	±2.4662E-4	0.98
E (PANi 8%)	7.25E-3	±3.4645E-4	0.98
F (PANi 11%)	7.97E-3	±1.3288E-4	0.99

This effect is extremely undesirable for many sensors because water vapour molecules are in competition with the analytes for the same interaction sites, perturbing the chemical interaction. Thus, for sensing application, in order to control or reduce the humidity effects, filters, cartridges or permeation tubes have to be used.

Unexpectedly **[41]**, when PANi/PHB fibrous sensors were used for measuring ammonia (1 ppm) in different conditions of environmental humidity, the response time dramatically changed: it was relatively long in anhydrous condition, with a few minutes of inertia before a significant change of current; on the contrary it was extremely fast when

measurements were carried out to higher relative humidity percentages (ranging between 10% and 70%). This effect was enhanced overall in F, that in 200 s (70% RH) achieved the same current value that F_{dry} (i.e. ΔI) achieved in more than 800 s (Figure 9). It is presumed that water molecules adsorbed on the surface of the fibrous scaffold facilitated the solvation of polar molecules or soluble in water, such as it happens in nature where the fibrous sensory structures protrude in aqueous matrices (even in the mammalian olfactory system) to keep in touch faster with the molecules of the surrounding environment.

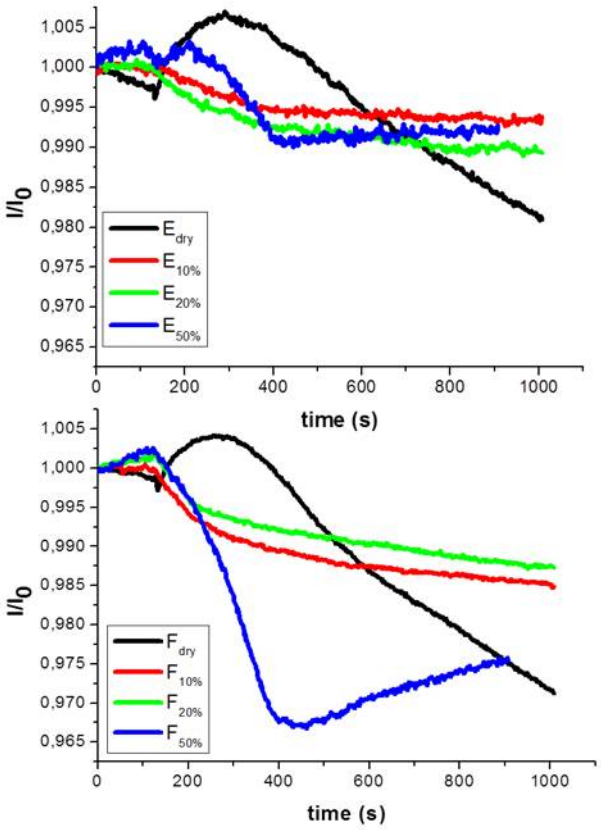

Figure 9. Comparison of the normalised transient responses of the sensors E (on the top) and F (on the bottom) to ammonia (1 ppm) under dry and variously humidified air (300 sccm), (V=+2 V).

Since ammonia is an electron-donor, when it interacts with PANi, deprotonation is expected to occur, transforming the emeraldine salt form into the insulating base form, then increasing the resistance value. A competitive mechanism (energetically favourable) to deprotonation can occur when ammonia reacts with PANi, (between N and H atoms of

PANi and NH_3, respectively), causing a complete symmetrisation of the chemical bonds and a lowering of the total energy of the polymer chain **[23]**. Instead of deprotonation, this mechanism increases the conductivity of the polymer: such an effect can be noticed in dry air when ammonia starts the interaction with the fibres (Figure 9). However, the response of sensor F, the most conductive one, to NH_3 as a function of gas concentration (ppb), showed a general decrease in current with increasing concentrations of analyte in the measurement chamber. The 90% equilibrium response was achieved after more than 20 min of gas flow in dry air. On the other hand, the response times to ammonia were shortened in moist air (Figure 9). Figure 10 depicts the sensor F transient responses when a defined concentration of ammonia (834 ppb) was cyclically flowed throughout the measurement chamber under 10% RH. The sensor showed both comparable responses and starting current recovery when the sensing gas was turned on, despite a slight drift of the sensor.

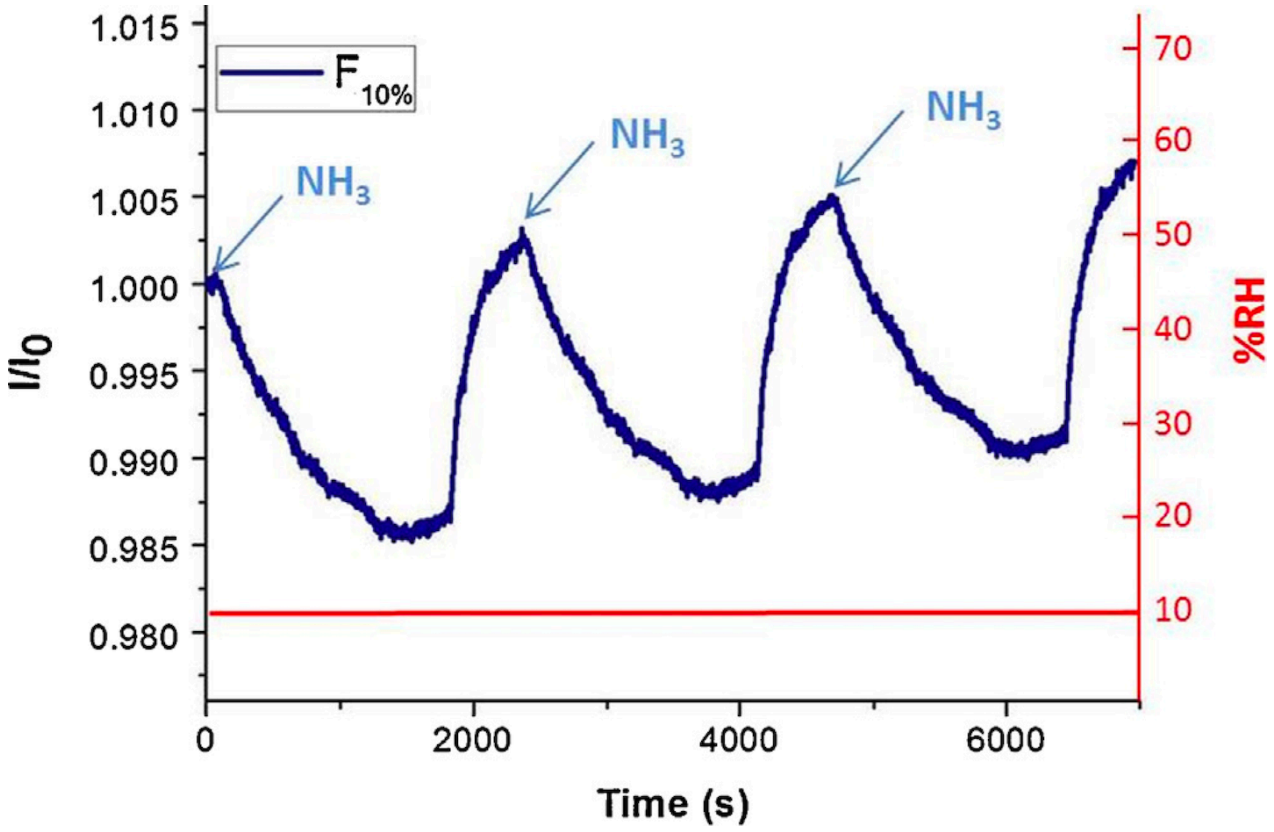

Figure 10. *Bi-plot* of three consecutive responses of F sensor, reported as normalised current (I/I_0) to the same concentration of NH3 (834 ppb) flowed throughout the measuring chamber (300 sccm) in 10% wet air (%RH) (V = +2 V).

Sensor sensitivity, too, calculated as the slope of each calibration curve at the lowest gas concentrations, resulted improved when humidity percentage increased too (Figure 11).

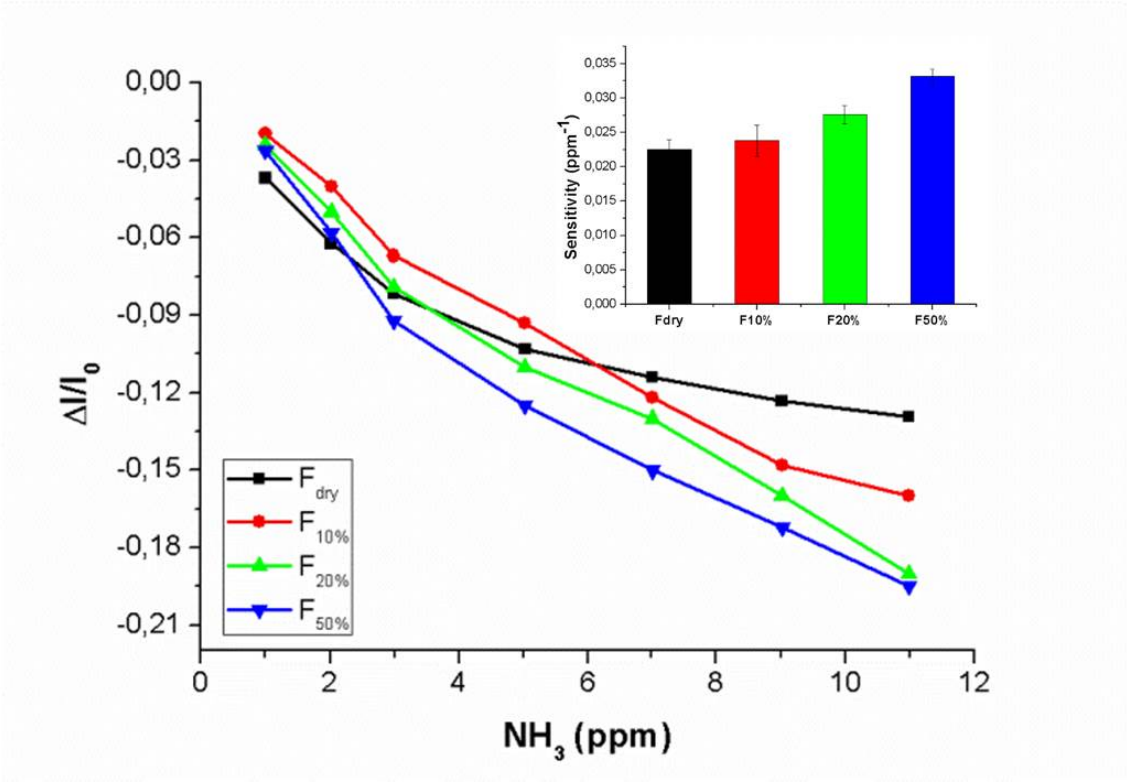

Figure 11. Response curves of F sensor to increasing concentrations of NH_3 when air ranged between dry and 50% wet (V=+2 V). The sensor sensitivity values were reported in the bar plot (inset).

Since TEA and AcAc are commonly used as chemical markers in odours smelling associated to specific phenomena, such as food spoilage (i.e. fish spoilage), monitoring their presence and concentration sounds consequently of outmost importance, for instance, in food quality applications. The response time of the chemosensors to a selected vapour pressure of triethylamine (TEA) and acetic acid (AcAc) decreased when the relative humidity increased. The sensor responses were compared and depicted in Figure 12: the very low current changes due to the VOCs interactions in dry air resulted increased when % RH also augmented. Therefore, as expected from literature, the current

of F sensor decreased, specifically of 0.3%, 0.9%, 34% and 68% when 0.03 p/p^0 TEA (where p and p^0 denote the vapour pressure and the saturated vapour pressure, respectively) flowed throughout the measuring chamber for 187 s under increasing humidity percentages, i.e. dry, 10%, 50% and 70%, respectively. Similarly, 0.03 p/p^0 AcAc flushing over the sensors for 450 s, increased the current of the sensor F 1.9%, 2.5%, 7.9% and 11.4% respectively. Since the sensors came to equilibrium after several tens of minutes (useless in sensors applications), only the transient response slope values were taken in consideration and calculated, thereby drastically reducing measurement time in a few minutes (Tab. 2).

Table 2. The slope values of the linear fitting of the first 100 seconds of measurements (except for acetic acid (*): after 100 seconds) to several analytes under different humidity percentages.

Analytes	E [I_{norm}/s](s^{-1})	St.Er.	R-sq	F [I_{norm}/s](s^{-1})	St.Er.	R-sq
NH_3 dry	$5.5962 \cdot 10^{-5}$	$\pm 2.296 \cdot 10^{-6}$	0.88	$3.4997 \cdot 10^{-5}$	$\pm 2.008 \cdot 10^{-6}$	0.84
NH_3 10%RH	$-2.3406 \cdot 10^{-5}$	$\pm 6.381 \cdot 10^{-6}$	0.93	$-4.8879 \cdot 10^{-5}$	$\pm 1.103 \cdot 10^{-6}$	0.96
NH_3 20%RH	$-3.2262 \cdot 10^{-5}$	$\pm 8.611 \cdot 10^{-7}$	0.95	$-4.9613 \cdot 10^{-5}$	$\pm 1.485 \cdot 10^{-6}$	0.92
NH_3 50%RH	$-5.8546 \cdot 10^{-4}$	$\pm 1.353 \cdot 10^{-6}$	0.95	$-1.6044 \cdot 10^{-4}$	$\pm 1.333 \cdot 10^{-6}$	0.99
TEA dry	$-8.9840 \cdot 10^{-6}$	$\pm 3.914 \cdot 10^{-7}$	0.93	$-1.4935 \cdot 10^{-5}$	$\pm 3.914 \cdot 10^{-6}$	0.93
TEA 10%RH	$-3.5050 \cdot 10^{-5}$	$\pm 5.568 \cdot 10^{-7}$	0.95	$-4.3751 \cdot 10^{-5}$	$\pm 3.914 \cdot 10^{-6}$	0.94
TEA 60%RH	$-1.7610 \cdot 10^{-2}$	$\pm 1.037 \cdot 10^{-5}$	0.99	$-1.8101 \cdot 10^{-2}$	$\pm 3.914 \cdot 10^{-6}$	0.98
TEA 70%RH	$-1.8670 \cdot 10^{-2}$	$\pm 2.160 \cdot 10^{-3}$	0.99	$-2.2041 \cdot 10^{-2}$	$\pm 3.914 \cdot 10^{-6}$	0.99
AcAc dry(*)	$4.7944 \cdot 10^{-5}$	$\pm 9.023 \cdot 10^{-7}$	0.94	$6.1092 \cdot 10^{-5}$	$\pm 8.851 \cdot 10^{-7}$	0,96
AcAc 10%RH(*)	$4.5399 \cdot 10^{-5}$	$\pm 9.081 \cdot 10^{-7}$	0.91	$6.9097 \cdot 10^{-5}$	$\pm 1.111 \cdot 10^{-6}$	0.96
AcAc 60%RH(*)	$1.1306 \cdot 10^{-4}$	$\pm 1.671 \cdot 10^{-6}$	0.96	$2.3265 \cdot 10^{-4}$	$\pm 2.36 \cdot 10^{-6}$	0.98
AcAc 70%RH(*)	$3.8888 \cdot 10^{-4}$	$\pm 1.287 \cdot 10^{-6}$	0.99	$3.9109 \cdot 10^{-4}$	$\pm 9.62 \cdot 10^{-7}$	0,99

Furthermore, the protracted exposure to the several analytes irreversibly changed sensors electrical performances. The chemical interactions of PANi with ammonia in a very humidified environment and for a long time, were supposed to dedope and change PANi chains conformation, modifying the electrical properties of the material. Such an effect is

suggested by Figures 9 where sensor to 50% RH, after 300 s under flow of ammonia (1 ppm), showed a sudden reversal trend of the current, despite of the regular tendency when the measurements were carried out under lower percentages. Similar effects were reported in Figure 12 when AcAc was flowed to 60% RH and more evident to 70% RH, when after a starting decreasing in current, an abrupt change of tendency reported an increasing current trend, as expected by the interaction between PANi and an acid. Indeed acetic acid vapours, wetting the surface of fibrous layer, were able to partially solve PHB, inducing a swelling of fibres (decrease in current) before interacting with PANi molecules and causing the likely current rise. For this reason, as regards the measurements related to AcAc, the linear fitting was calculated after the first 100 seconds of response (Table 2), that is when the sudden change of the current trend occurred. All sensors could be recovered after a flow of humid air to the same value percentage of the measurement when measurements were no longer than 6 min. The desorption time (data not shown) suggested that the wet gas carriers carried away more quickly the analytes from fibres. All sensors were tested for more than one year, showing stability in morphology and electrical parameters, with a slight tendency to decrease in resistance probably due to irreversible moisture adsorption. After each set of measurements, they were stored in small boxes in the dark and dry environment before reuse. After 1 year, the resistance value of F, the most conductive sensor, resulted increased by ~6.3%. This result could be also due to a potential starting biodegradation of PHB, responsible of changing the proportion of the polymer within the fibres, but further investigation concerning the effects of the biodegradation (morphological and electrical) on the sensors are still in progress.

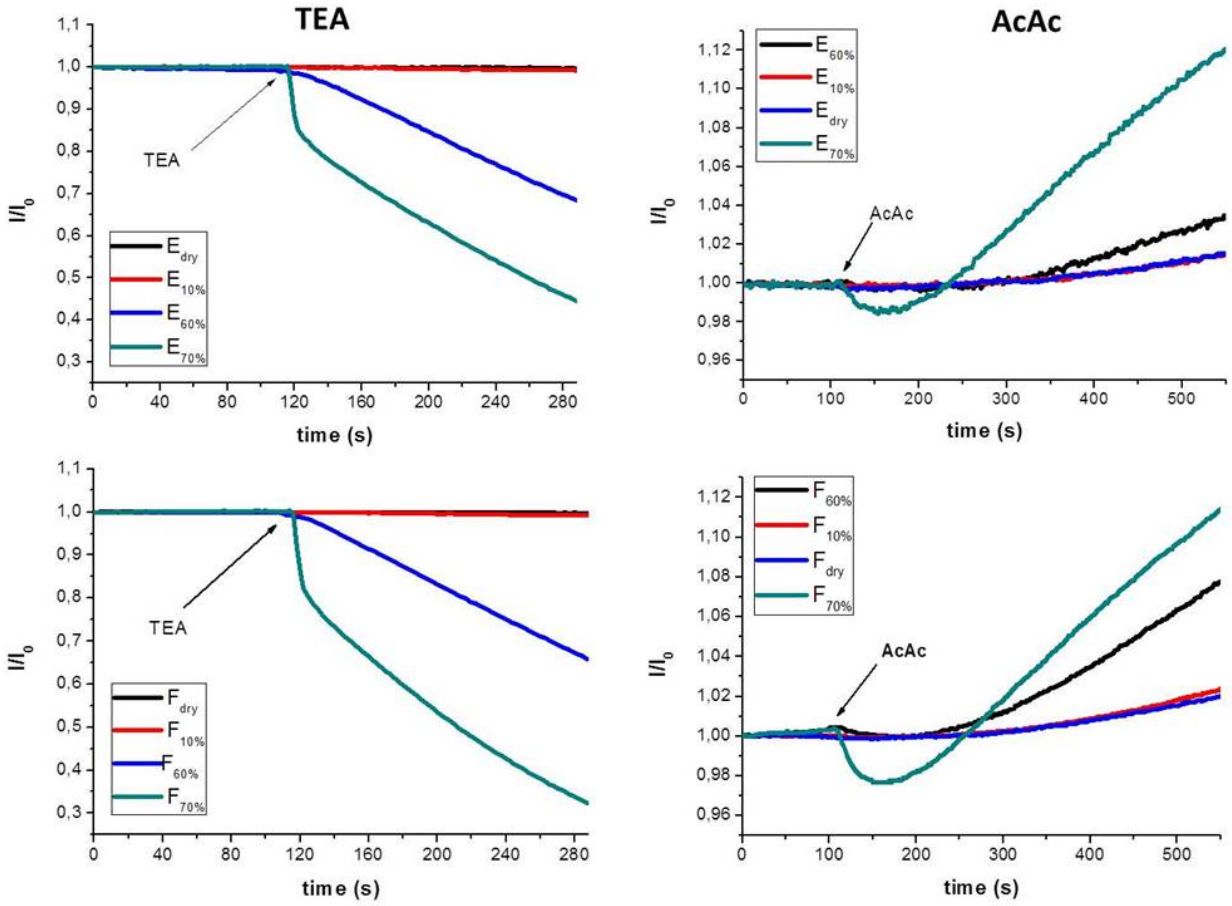

Figure 12. Comparison of the normalised transient responses of the sensors E (on the top) and F (on the bottom) to TEA (0.03 p/p^0) and AcAc (0.03 p/p^0) under dry and variously humidified air (300 sccm).

4.CONCLUSIONS

Nanofibres composed of PANi/PHB blends were prepared and deposited through electrospinning on chemoresistors in order to be investigated as potential biodegradable chemical sensors. The electrospinning technology was used in order to design and obtain materials with high performance sensing features. PANi and PHB polymers were selected for their crucial remarkable characteristics, such as gas sensitivity and biodegradability, respectively. Six nanofibrous samples with increasing PANi/PHB mass ratio were manufactured and characterised. Thus, networks of continuous nanofibres with high porosity and covering the sensing area of the interdigitated electrodes were observed for each polymer solution. The increase in PANi concentration created a sharper distribution of the diameter sizes (~200 nm) as well as rougher and lumpy fibres. TEM

pictures reported a more homogeneous distribution of PANi within the PHB fibres, especially at higher concentrations, as confirmed by the analysis of electrical parameters. The potentials of such blended polymers were exploited, focusing the attention on the influence of humidity on the features of the resulting chemosensors. Ammonia in trace was measured in dry air and at different percentages of relative humidity, in order to evaluate the influence of PHB in the interaction of PANi with the gas in possible applications. Similarly, both acidic and basic volatile organic compounds were detected at different values of environmental humidity, until 70% RH. The peculiar structure of the nanofibrous layer as well as the physicochemical properties of PANi/PHB, enabled ammonia and VOCs detection at high percentages of humidity, thus decreasing the response time and, specifically for VOCs, increasing the sensor responses. Moisture is generally an extremely undesirable environmental parameter for many sensors. In the case of electrospun PANi/PHB chemosensors here proposed, the natural strategy of sensing is mimicked, where an aqueous film over cilia (here represented by the nanofibres) is used to solve interacting molecules with surface thus facilitating the chemical interactions. This findings suggest the possibility for such sensors to be used in applications where monitoring strongly moist environments is required (e.g. food packaging, breath analysis, skin perspiration, soil, air in different environmental conditions, etc.), without any need to abate or reduce water vapours content. The resulting sensing features suggest the chance to integrate these electrospun chemosensors within smart devices usable anytime and anywhere and capable of providing qualitative and quantitative information about pollutants without representing a significant additional source of pollution to the environment once worn out. Noticeably, a humidity sensor will be necessary, in these cases, to relate the responses of sensors to the amount of analytes of interest. In laboratory, sensors have worked for more than one year showing stability in both morphology and electrical parameters. They were primarily designed on purpose to be biodegradable and then to fabricate an eco-friendly sensing system, but they also resulted desirable for their low cost, ease of measurement, low power consumption, dimension and good performance at room temperature. Further

investigations are currently ongoing on both their sensing features and the related timing of biodegradation under natural conditions.

REFERENCES

1) http://www.who.int/mediacentre/news/releases/2014/air-pollution/en/(*25/03/ 2014*).
2) DA. Vallero, Fundamentals of Air Pollution, Fifth Edition Elsevier, USA, 2014 pp. 0-996, *ISBN:978-0-12-401733-7.*
3) SS. Nadadur, JW Hollingsworth, Air Pollution and Health Effects, in Molecular and Integrative Toxicology Series, Springer-Verlag, London, 2015 pp.0-439, *ISBN. 10.1007/978-1-4471-6669-6*.
4) M. Irimia-Vladu, ED. Głowacki, G. Voss , S. Bauer and NS. Sariciftci, Green and biodegradable electronics, Mater. Today 15 (2012) 340-346.
5) M. Irimia-Vladu, "Green" electronics: biodegradable and biocompatible materials and devices for sustainable future, Chem. Soc. Rev. 43 (2014) 588-610.
6) DH. Kim, N. Lu, R. Ma, YS. Kim, RH. Kim, S. Wang, et al. Epidermal Electronics Science 333 (2011) 838–843.
7) AA. Shah, F. Hasan, A. Hameed, S. Ahmed, Biological degradation of plastics: A comprehensive review, Biotechnol. Adv. 26 (2008) 246-265.
8) B Singh, N Sharma. Mechanistic implications of plastic degradation Polym Degrad Stability 93 (2008) 93 561-584
9) A. Macagnano, E. Zampetti**,** E. Kny, Electrospinning for high performance sensors, in Nanoscience and Technology, Springer International Publishing, Switzerland, 2015, pp.0-329 *ISBN 978-3-319-14406-1.*
10) P. Humpolicek, V. Kasparkova, P. Saha, J. Stejskal, Biocompatibility of polyaniline, Synt. Met. 162 (2012) 722–727.
11) Z. Kucekova, P. Humpolicek, V. Kasparkova, T. Perecko, M. Lehocký, I. Hauerlandová, P. Sáhab, J. Stejskale, Colloidal polyaniline dispersions: Antibacterial activity, cytotoxicity and neutrophil oxidative burst, Colloids Surf. B Biointerfaces 116 (2014) 411–417.
12) LE. Ibarra, L. Tarres, S. Bongiovanni, CA. Barbero, MJ. Kogan, VA. Rivarola, ML. Bertuzzi, EI. Yslas, Assessment of polyaniline nanoparticles toxicity and teratogenicity in aquatic environment using Rhinella arenarum model, Ecotoxicol. Environ. Saf. 114 (2015) 84–92.
13) EI. Yslas, LE. Ibarra, DO. Peralta, CA. Barbero, VA. Rivarola, ML. Bertuzzi, Polyaniline nanofibres: acute toxicity and teratogenic effect on *Rhinella arenarum* embryos, Chemosphere 87 (2012) 1374-1380.
14) S. Virji, J. Huang, RB. Kaner, and BH. Weiller, Polyaniline Nanofibre Gas Sensors: Examination of Response Mechanisms, Nano Lett. 4 (2004) 491-496.
15) H. Bai, G. Shi, Gas Sensors Based on Conducting Polymers, Sensors 7 (2007) 267-307.
16) CT. Laurencin, AM. Ambrosio, MD. Borden, JA. Cooper Jr., Tissue Engineering: Orthopedic Applications, Ann. Rev. Biomed. Eng. 1 (1999) 19-46.

17) P. Gibson, HL. Shreuder-Gibson, D. Rivin, Transport properties of porous membranes based on electrospun nanofibres, Colloids Surf. A 187–188 (2001) 469-481.
18) X. Wang, C. Drew, SH. Lee, KJ. Senecal, J. Kumar, LA. Samuelson, Electrospun Nanofibrous Membranes for Highly Sensitive Optical Sensors, Nano Lett. 2 (2002) 1273–1275.
19) S. Ramakrishna, K. Fujihara, W-E. Teo, T. Yong, Z. Ma, R. Ramaseshan, Electrospun nanofibres: solving global issues, Mater. Today 9 (2006) 40-50.
20) A. Macagnano, E. Zampetti, S. Pantalei, F. De Cesare, A. Bearzotti, K. Persaud, Nanofibrous PANI-based conductive polymers for trace gas analysis,Thin Solid Films 520 (2011) 978–985.
21) Z. Yuxi, JJ. Kim, D. Chen, HL. Tuller and GC. Rutledge, Electrospun Polyaniline Fibres as Highly Sensitive Room Temperature Chemiresistive Sensors for Ammonia and Nitrogen Dioxide Gases, Adv. Funct. Mater. 24 (2014) 4005–4014.
22) W. Serrano, A. Meléndez, I. Ramos and NJ. Pinto, Sensor response of electrospun poly(lactic acid)/polyaniline nanofibres to aliphatic alcohol vapours of varying sizes, Sensors (IBERSENSOR), 2014 IEEE 9th Ibero-American Congress on, IEEE Bogota 15-18 Oct. 2014, pp. 1-4, *ISBN. 978-1-4799-6835-0, DOI. 10.1109/IBERSENSOR.2014.6995537.*
23) W. Li, DM. Jang, SY. An, D. Kim, S-K. Hong, H. Kim, Polyaniline–chitosan nanocomposite: High performance hydrogen sensor from new principle, Sens. Actuat. B-Chem. 160 (2011) 1020–1025.
24) W. Hu, S. Chen, Z. Yang, L. Liu, H. Wang, Flexible Electrically Conductive Nanocomposite Membrane Based on Bacterial Cellulose and Polyaniline, J. Phus. Chem. B115 (2011) 8453-8457.
25) YA. Ismail, JG. Martìnez, TF. Otero, Fibroin/Polyaniline microfibrous mat. Preparation and electrochemical characterization as reactive sensor, Electrochim. Acta 123 (2014) 501-510.
26) K. Low, N. Chartuprayoon, C. Echeverria, C. Li, W. Bosze, NV. Myung, J. Nam, Polyaniline/poly(ε-caprolactone) composite electrospun nanofibre-based gas sensors: optimization of sensing properties by dopants and doping concentration, Nanotechnology 25 (2014) 115501.
27) J. Ackermann, S. Müller, A. Lösche, T. Bley, W. Babel, Methylobacterium rhodesianum cells tend to double the DNA content under growth limitations and accumulate PHB, J. Biotechnol. 39 (1995) 9–20.
28) PLB. Araujo, CRPC. Ferreira, ES. Araujo, Biodegradable conductive composites of poly(3-hydroxybutyrate) and polyaniline nanofibres: Preparation, characterization and radiolytic effects, eXPRESS Polymer Letters 5 (2011) 12–22.
29) M. Matsuguchi, A. Okamoto, Y. Sakai, Effect of humidity on NH3 gas sensitivity of polyaniline blend films, Sensor. Actuat. B-Chem. 94 (2003) 46–52.
30) J. Janata, M. Josowicz, Conducting polymers in electronic chemical sensors, Nat. Mater. 2 (2003) 19-24.
31) S. Wolf, RN. Tauber, Silicon Processing for VLSI, Vol. 1,:Process Technology, Lattice Press, USA, 2000, pp. 0-960, *ISBN-13:978-0961672133*.

32) Z. Li, C. Wang, Effects of Working Parameters on Electrospinning, in One-Dimensional Nanostructures, Springer Berlin Heidelberg 2013, pp. 15-28, *DOI: 10.1007/978-3-642-36427-3_2.*
33) W. Liu, M. Graham EA. Evans, DH. Reneker, H Darrell, Poly(Meta-Phenylene Isophthalamide) Nanofibres: Coating and Post Processing, J. Mater. Res. 17 (2002) 3206-3212.
34) AP. Golin, Humidity Effect on the Structure of Electrospun Core-Shell PCL-PEG Fibers for Tissue Regeneration Applications" (2014), Electronic Thesis and Dissertation Repository, Paper 1999,
http://ir.lib.uwo.ca/etd/1999.
35) QL. Hao, V. Kulikov, VA. Mirsky, Investigation of contact and bulk resistance of conducting polymers by simultaneous two- and four-point technique, Sensor. Actuators. B Chem. 94 (2003) 352
36) GF. Li, C. Martinez, J. Janata, JA. Smith, M. Josowicz, S. Semancik, Effect of morphology on the response on polyaniline-based conductometric gas sensors: Nanofibres vs thin films, Electrochem. Solid St. 7 (2004) H44-H48
37) Z. Ma, M. Kotaki, S. Ramakrishna. Surface modified nonwoven polysulphone (PSU) fibre mesh by electrospinning: A novel affinity membrane, J. Membrane Sci. 272 (2006) 179-187

Figures' Captions

Figure 1. Optical micrographs of the nanofibrous layers called A (*a*) and F(*b*), respectively, coating microscope glass slides; (*c*) a picture of CNR-IIA home-made electrospinning equipment comprising a rotating collector where transducers were placed for deposition. The yellow arrow points to an interdigitated electrode after an electrospun deposition, where a rectangular area was magnified by optical micrograph (red framed).

Figure 2. SEM micrographs show PANi/PHB nanofibres coating silicon wafers at increasing PANi mass ratios (A:1.4%, D:5.45%, E: 8%, F:11%).

Figure 3. TEM micrographs show A, D, E and F samples, contrasted with uranyl acetate.

Figure 4. Current-Voltage curves of all the PANi/PHB sensors (A, B, C, D, E, F) between -2 V and +2 V in dry air.

Figure 5. Electrical parameters of the investigated chemosensors; a) bar plot of electrical resistance values of the nanofibrous sensors; b) curve fitting of the electrical resistance values vs PANi/PHB mass ratio in percentage.

Figure 6. Response curves of PANi/PHB nanofibrous chemosensors to increasing percentages of relative humidity (% RH), ranging between 10%-60% (V=+2 V). For each sensor, the current values (I) were normalized to the starting current values (I_0) before the measuring, in order to be compared.

Figure 7. *Top:* WCA pictures of the A, D and F samples captured by a digital microscope and an optical microscope. *Bottom:* bar-plot of the sensitivity (*S*) of the sensors to water vapours concentrations (*ppm*), measured as the slope of the linear fitting of the normalized response curve of each sensor (I/I_0), i.e. $S = (I/I_0)/C$, where *C* is the analyte concentration

Figure 8. Current-Voltage curves (-3 V ;+ 3 V) of the sensors named E and F under flow of both dry and humidified air.

Figure 9. Comparison of the normalized transient responses of the sensors E (on the top) and F (on the bottom) to ammonia (1 ppm) under dry and variously humidified air (300 sccm), (V=+2 V).

Figure 10. Three consecutive responses of F sensor, reported as normalized current (I/I_0) to the same concentration of NH3 (834 ppb) flowed throughout the measuring chamber (300 sccm) in 10% wet air (V=+2 V).

Figure 11. Response curves of F sensor to increasing concentrations of NH_3 when air ranged between dry and 50% wet (V=+2 V). The sensor sensitivity values were reported in the bar plot (inset).

Figure 12. Comparison of the normalized transient responses of the sensors E (on the top) and F (on the bottom) to TEA (0.03 p/p^0) and AcAc (0.03 p/p^0) under dry and variously humidified air (300 sccm).